PHYSICAL REVIEW D **73,** 085012 (2006)

Creation of defects with core condensation

Nuno D. Antunes

Center for Theoretical Physics, University of Sussex, Falmer, Brighton BN1 9WJ, United Kingdom

Pedro Gandra, Ray J. Rivers, and A. Swarup

Blackett Laboratory, Imperial College, London SW7 2BZ, United Kingdom

(Received 30 January 2006; published 28 April 2006)

Defects in superfluid ^{3}He, high-T_c superconductors, QCD color superfluids, and cosmic vortons can possess (anti)ferromagnetic cores, and theirgeneralizationss. In each case there is a second-order parameter whose value is zero in the bulk which does not vanish in the core. We examine the production of defects in the simplest $1+1$ dimensional scalar theory in which a second-order parameter can take nonzero values in a defect core. We study in detail the effects of core condensation on the defect production mechanism.

DOI: 10.1103/PhysRevD.73.085012 PACS numbers: 03.70.+k, 03.65.Yz, 05.70.Fh

I. INTRODUCTION

Since phase transitions take place in a finite time, causality guarantees that correlation lengths remain finite. If the symmetry breaking permits nontrivial homotopy groups the frustration of the order parameter fields is resolved by the creation of topological defects to mediate between the different ground states. Since defects are, in principle, observable, they provide an excellent experimental tool for determining how transitions occur.

Zurek [1,2] and Kibble [3] originally suggested that causality alone is sufficient to bound the initial density of defects arising in a continuous transition, whether in condensed matter or quantum field theory. The analysis is very general, and depends on the fact that there is a maximum speed (e.g. the speed of light or the speed of sound) at which the system can become ordered. The Zurek-Kibble (ZK) causal arguments can be quantified in many variants, and we will not rehearse them here. It is sufficient to consider a system with critical temperature T_c, cooled through that temperature at a rate

$$\frac{1}{T_c}\frac{dT}{dt}\bigg|_{T_c} = -\frac{1}{\tau_Q}, \tag{1}$$

thereby defining the quench time τ_Q. The prediction is that, if $\bar{\xi}$ is the defect separation at the time of defect formation, then

$$\bar{\xi} = f\xi_0\left(\frac{\tau_Q}{\tau_0}\right)^{\sigma} \gg \xi_0, \tag{2}$$

where τ_0 is the relaxation time for short wavelength modes and ξ_0, also determined from the microscopic details of the system, characterizes the size of cold defects. The coefficient f is an undetermined efficiency factor, taken to be $O(1)$, but anticipated to be greater than unity.

We term σ the ZK characteristic index. Its mean-field values are typically $\sigma = 1/3$ for relativistic systems and $\sigma = 1/4$ for strongly damped nonrelativistic systems. Experiments on a range of condensed-matter systems (superfluid ^{3}He [4,5], high-T_c superconductors [6,7], Josephson tunnel junctions (JTJs) [8,9]) give results that are commensurate with (2).

This may seem paradoxical in that subsequent analytic approximations [10,11] and numerical simulations [12–14] have shown that, for simple systems, the scaling behavior of (2) is understood, not so much in terms of causal bounds, but in terms of the instabilities of the time-dependent Ginzburg-Landau (TDGL) theory, whose dissipative behavior controls which regime we are in. However, where scaling is appropriate it is found that causality arguments identify the correct engineering dimensions for the scaling behavior of defect densities [11,14] and (2) survives [15].

For symmetry breaking of local gauge theories the result (2) is not complete because of the freezing in of long wavelength modes of the gauge fields [16]. However, for the high-T_c experiments of [6,7] and the JTJs of [8,9]) the effect of this additional mechanism is small and we shall ignore it, given that it does not occur for the simple model that we shall solve numerically later.

For each of the condensed-matter systems listed above the relevant topological defects are vortex lines (strings). Again, in the context of the early universe, strings (cosmic strings) are the almost inevitable consequence of symmetry breaking in the most obvious extensions of the standard model for electroweak unification [17]. Observation has suggested the possible existence of cosmic strings [18–20] but, as yet, the evidence is not compelling.

Most simply, for both condensed matter and the early universe, the most studied and best understood strings arise from the breaking of a global or local $U(1)$ symmetry, in which the order parameter can be represented by a single complex scalar field. In such cases the structure of the vortex is quite simple, with a trivial core, in the center of which the order parameter vanishes, restoring the $U(1)$ symmetry there. That is, a string is a simple tube of false vacuum or ground state, trapping flux if the symmetry is local. Although this is appropriate for the phases of the

condensed-matter systems for which experiments have been performed, it is a simplification since both superfluid ^{3}He and high-T_c superconductors have order parameters $\vec{\Phi}$ with several components. The unstable ground state (''false vacuum'') corresponds to $\vec{\Phi} = 0$. We can separate the components of $\vec{\Phi}$ into two types $\vec{\Phi} = (\vec{\phi}, \vec{\eta})$ so that, in bulk, the $\vec{\phi}$ fields condense (i.e. are nonzero), whereas the $\vec{\eta}$ fields do not. For any defect this characterizes the situation in its exterior and, for a ''normal'' defect, *both* $\vec{\phi}$ and $\vec{\eta}$ are zero in the core. However, in some parts of parameter space it may require less energy to produce defects with ''abnormal'' cores, in which $\vec{\phi} = 0$, but the $\vec{\eta} \neq 0$. The existence of defects inside which the $\vec{\eta}$ fields condense is not a question of topology, merely one of energetics.

This is the case for superfluid ^{3}He $-$ B with its nine complex order parameters, for which there is experimental evidence for superfluid ^{3}He $-$ B vortices with ferromagnetic ^{3}He $-$ A cores [21,22]. Also, this phenomenon has been predicted to occur in the idealized $SO(5)$ model [23,24] of high-temperature superconductivity, where, for appropriate doping, the cores of the conventional Abrikosov vortices are antiferromagnetic. There has been recent experimental evidence to support this theoretical picture [25–29].

This is not just a phenomenon of condensed-matter physics. It has been argued [30–32] that such strings also occur in the so-called color superconducting phase of QCD, that is believed to be realized when the baryon density is a few times larger than nuclear density [33], and hence in neutron stars. In fact, that such a phenomenon can occur in relativistic systems was first discussed by Witten [34] on looking at generalizations of cosmic strings. His model is the simplest of all that is compatible with early universe cosmology: consider a two-component system described by two complex scalar fields (ϕ, η) with an approximate $U(2)$ symmetry. If the $U(2)$ symmetry between fields ϕ and η is explicitly broken down to $U(1) \times U(1)$, the ϕ condensation might be energetically more favorable than η condensation, and the ground state will be given by $\langle\phi\rangle \neq 0$ and $\langle\eta\rangle = 0$. As intimated above, this system permits ϕ vortices characterized by the phase of ϕ field varying by an integer multiple of 2π as one traverses a contour around the vortex core. Witten showed that, if the approximate $U(2)$ symmetry is broken only weakly, the η field may condense inside the core of the ϕ string, breaking the corresponding $U(1)$ symmetry in the core.

One consequence of this ''core condensation'' is that [35–38] it provides a way to stabilize a string loop against shrinking, as would normally be the case because of the string tension. The condensed-matter counterpart to Witten's model of approximate $U(2)$ symmetry breaking is in two-component Bose-Einstein condensates (BECs) [39], for which both core condensation and this stabilization may already have been seen.

Most of the work cited above has addressed the static properties of defects with core condensation. In this paper we are interested in the dynamics of the creation of such defects. Insofar as the scaling behavior of (2) is truly a consequence of causality we would expect it to be equally true for defects with and without core condensation. However, it may not be so simple in that one consequence of core condensation is that the interactions between vortices can be drastically altered by the presence of nontrivial cores [40]. In the following sections we shall consider the simplest model permitting core condensation, to check whether the formation accords with the simple Kibble-Zurek scaling laws in τ_Q of (2).

II. THE $O(2) \rightarrow Z_2 \times Z_2 \rightarrow Z_2$ MODEL IN 1D

Our model is a simplified version of more realistic dissipative systems, such as the Ginzburg-Landau description [41] of high-T_c superconductors. However, with the early universe in mind we extend it to a relativistic underdamped model when appropriate.

Specifically, let us consider the symmetry breaking $O(2) \rightarrow^{ESB} Z_2 \times Z_2 \rightarrow^{SSB} Z_2$ in one dimension, where ESB denotes explicit symmetry breaking by the introduction of terms in the action and SSB denotes spontaneous symmetry breaking. We consider a free energy of the form

$$F = \int dx[\tfrac{1}{2}[(\partial_x\phi)^2 + (\partial_x\eta)^2] + V(\phi, \eta)], \qquad (3)$$

where

$$V(\phi, \eta) = \frac{1}{2}a(T)\phi^2 + \frac{1}{2}a(T)\beta\eta^2 + \frac{b}{4}(\phi^2 + \eta^2)^2 + \frac{a^2}{4b} \qquad (4)$$

for which we have chosen to implement the ''phase transition'' explicitly through the Landau form $a(T) = -a'(1 - T/T_c)$, where $a' > 0$. The fact that there is no true transition in one dimension is irrelevant for the rapid changes in temperature that we shall consider [12].

When $\beta = 1$ F possesses $O(2)$ symmetry, and we can take ϕ and η to be the real and imaginary parts of a complex field Φ. There is a minor complication in that, if we fix the phase of Φ to be zero, say, at infinity, making space S^1, the winding number of the phase is a conserved charge. However, the configurations with nonzero charge are Skyrmions, and not the defects of relevance to the ZK scenario, of which none exist in the absence of topological charge when there are no fixed boundary conditions.

The $O(2)$ is broken explicitly to $Z_2 \times Z_2$ when $\beta \neq 1$, which will be the case of interest for defect formation. In 1D, the defects are kinks. For example, to convert F of (3) into an $SO(5)$ model for high-T_c along the lines of [41] we elevate ϕ into the two-component complex field that couples to the electromagnetic field, and elevate η to the three-component Néel vector of antiferromagnetism. A similar transmutation would recreate a model like Witten's. In this

regard, we note that the potentials presented in the literature are not quite identical in the way the different sectors couple. They only become so on imposing nonlinear constraints (e.g. $\vec{\phi}^2 + \vec{\eta}^2 = f^2$), as in [41]. At an effective level this can make little difference to the statics of defects (e.g. [42]), but for the dynamics we revert to the more fundamental linear sigma model of (3), modeled on [42,43]. Phase transitions leading to kinks and walls with core condensation and displaying repulsive interactions were considered in the context of a $S_5 \times Z_2 \rightarrow S_3 \times S_2$ theory in [44]. In that case the authors were concerned mostly with the long-time behavior of the system after the transition. In particular, significant changes to the scaling behavior of domain wall networks were observed as well as the formation of defect lattices as the final product of the evolution. Here we will concentrate on the period straight after the transition, namely, on the process of defect formation, rather than on the long-time dynamics.

The properties of the translation invariant configurations that minimize the free energy above depend on the value of β. Defining $\phi_0^2 = -a/b$ and $\eta_0^2 = -\beta a/b$ we have that, for $\beta > 1$,

$$F[\phi_0, 0] > F[0, \eta_0], \qquad \beta > 1 \tag{5}$$

corresponding to a ground state with $\phi(x) = 0$.

For $0 < \beta < 1$ the opposite relation holds

$$F[\phi_0, 0] < F[0, \eta_0], \qquad 0 < \beta < 1 \tag{6}$$

and the preferred ground-state configuration is now $\eta(x) = 0$, $\phi^2(x) = \phi_0^2$. For $\beta < 0$, the case corresponding to Eq. (5) holds again, as β is now negative and η is therefore constrained to be zero.

A. Kink solutions

We will concentrate on the $0 < \beta < 1$ regime and consider kinklike solutions that minimize the action in Eq. (3) for the set of boundary conditions $\phi(-\infty) = -\phi_0$, $\eta(-\infty) = 0$ and $\phi(+\infty) = \phi_0$, $\eta(+\infty) = 0$. For any value of β in this region the free energy is always stationary for the straightforward kink solution obtained by setting

$$\phi(x) = \phi_0 \tanh(l_k x), \qquad \eta(x) = 0, \tag{7}$$

where $l_k = (-a/2)^{1/2}$ is the kink size. The free energy of this configuration is β independent and given by

$$F_k = \frac{2\sqrt{2}}{3} b^{1/2} \phi_0^3. \tag{8}$$

It is possible that for certain values of β other stable configurations exist with a lower free energy [42,43]. It turns out that, for this particular system, we were able to find such solutions analytically.

Any static solution obeys the time-independent equations of motion derived from the free-energy Eq. (3):

$$\partial_x^2 \phi = a\phi + b(\phi^2 + \eta^2)\phi, \tag{9}$$

$$\partial_x^2 \eta = \beta a \eta + b(\phi^2 + \eta^2)\eta. \tag{10}$$

We start by assuming that $\phi(x)$ has the usual kink profile

$$\phi(x) = \phi_0 \tanh(x/l), \tag{11}$$

where l, the size of the core can now depend on β. The trivial kink profile with $l_k = \sqrt{-2/a}$ and $\eta = 0$ is obviously a solution for all values of β. In order to find other possible solutions, we assume $\eta(x) \neq 0$ and replace the general kink profile (with arbitrary core size l) into the equation for ϕ, Eq. (9). Solving in terms of η we obtain:

$$\eta(x) = \phi_0 \left(1 + \frac{2}{al^2}\right)^{1/2} \frac{1}{\cosh(x/l)}. \tag{12}$$

Demanding that this result satisfies the second equation, Eq. (10), we obtain an explicit expression for the kink core size

$$l = \frac{1}{\sqrt{-a}} \frac{1}{\sqrt{1-\beta}} = \frac{l_k}{\sqrt{2-2\beta}}. \tag{13}$$

The full solution is then given by

$$\phi(x) = \phi_0 \tanh(x/l), \tag{14}$$

$$\eta(x) = \pm \phi_0 \sqrt{2\beta - 1} \frac{1}{\cosh(x/l)}. \tag{15}$$

Note that we have included the two possible signs for the η field. In general, for each choice of ϕ profile, there will be two allowed symmetric configurations for η. We will refer to solutions for which ϕ interpolates between $-\phi_0$ and ϕ_0 as x goes from $-\infty$ to ∞ as kinks. These can be positively of negatively charged, depending on whether η is positive or negative. Conversely, antikinks will have $\phi(-\infty) = \phi_0$ and $\phi(\infty) = -\phi_0$. We will say an antikink has negative charge if $\eta > 0$ and positive charge otherwise. This convention for the charge signs for kinks and antikinks corresponds to the winding direction of the solution in the (ϕ, η plane, mimicking the $U(1)$ charge definition in the $\beta \rightarrow 1$ limit. As we will see below, the interaction potential between kinks and antikinks will depend on their charges, as defined above.

The free energy of the nontrivial kink profile can be evaluated explicitly, being given by

$$F = F_k \sqrt{2-2\beta} (\tfrac{1}{2} + \beta), \tag{16}$$

where F_k the energy of the $\eta = 0$ solution as defined in Eq. (8). Such a kink is rather like a slice through a configuration known as a ''dark-bright vector soliton'' in two-component BEC [45], which consists of a domain wall formed by one condensate with the second condensate confined to the wall's center. The difference lies in the fact that the BEC condensate obeys nondissipative Gross-Pitaevskii equations, rather than the (relativistic) dissipa-

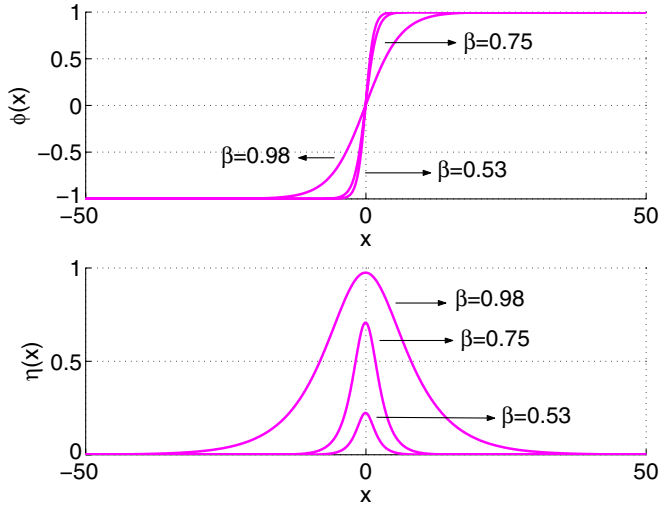

FIG. 1 (color online). Profiles of $\phi(x)$ and $\eta(x)$ for several values of $\beta > 0.5$, $a = -1.0$, and $b = 1.0$.

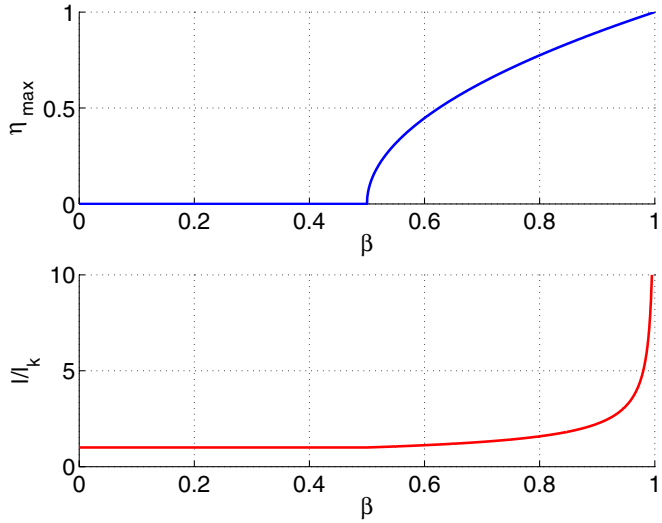

FIG. 3 (color online). Maximum value of $\eta(x)$ and core-length of the most stable configuration versus β.

tive TDGL equation appropriate to condensed matter and the early universe.

The above expressions for the fields' profiles and the free energy of the nontrivial solution are defined only for $\beta > \beta_c$, where $\beta_c = 0.5$, a value independent of the parameters of the theory. For β above the critical value we have that $F < F_k$, the free energy of the nontrivial solution is smaller than that of the $\eta = 0$ kink. In this region of parameter space the configuration in Eqs. (11) and (12) is energetically more stable and should be more likely to form as the outcome of a phase transition. As $\beta \to \beta_c^+$ this solution converges smoothly to the trivial kink profile, with $l \to l_k$, $\eta \to 0$, and $F \to F_k$. For $\beta < \beta_k$, Eq. (7) corresponds to the single valid solution. These points are illustrated in Figs. 1–3. In Fig. 1 we show several field profiles in the $\beta > \beta_c$ regime. As β approaches its critical value the size of the kink core decreases tending to l_k, and the magnitude of the peak of η goes to zero. In Fig. 2 we have the free energy of the most stable configuration, for β in the interval (0, 1). Finally, in Fig. 3 we show, for the most stable configuration, the maximum value of η and the size of the kink core. As expected, both these and the free energy are constant below β_c. It is interesting to note that while all these quantities are continuous at β_c, their derivatives behave in different ways. In particular, $F'(\beta)$ is continuous throughout the interval (0, 1), whereas the core size has finite discontinuous derivative at β_c and $\eta_{\max}$ has diverging derivative at β_c^+.

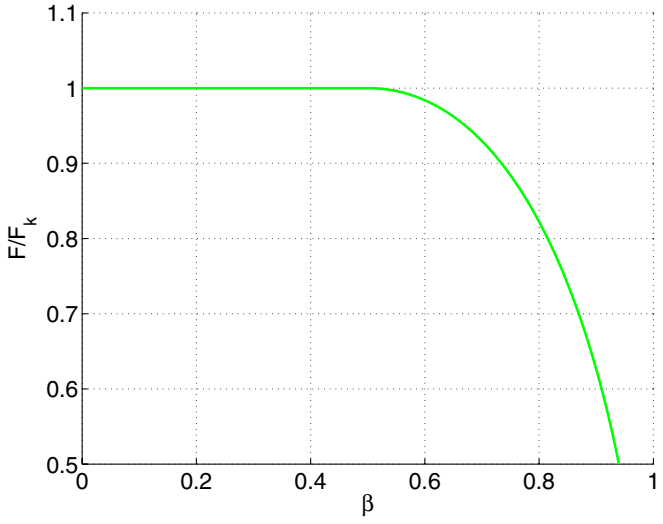

FIG. 2 (color online). The free energy of the most stable kink configuration against β, normalized by the energy of the $\eta = 0$ kink.

B. Kink/antikink interaction

The problem we want to address here is to determine what happens when a kink and an antikink are put in the vicinity of each other. For the trivial profiles corresponding to $\beta < 0.5$, it is well known that a kink and antikink attract each other with a force that decreases exponentially with the separation of the cores. In a setting where kinks and antikinks form as a consequence of a phase transition, this allows for pair annihilation processes. In our case, because of the presence of the extra field, kinks can have two distinct charges and it is reasonable to expect these to play a role in their interaction. If we imagine a kink/antikink pair with the same charge in the limit $\beta \sim 1$, the result is a configuration close to a "springy" $U(1)$ winding. The $U(1)$ spring will tend naturally to "stretch" itself, corresponding, in terms of the kink/antikink pair, to a repulsive interaction. The opposite reasoning suggests that kinks and antikinks with symmetric charges should attract each other.

In order to check this scenario and obtain effective interaction potentials we followed the gradient flow ap-

proximation [46]. This consists in setting up an initial kink/antikink configuration and evolving it numerically according to the first-order equation of motion corresponding to the free energy in Eq. (3):

$$\partial_t \phi_a = \partial_x^2 \phi_a - \frac{\partial V}{\partial \phi_a}, \tag{17}$$

where the index a runs from 1 to 2 with $\phi_1 = \phi$ and $\phi_2 = \eta$. This forces the solution to be locally on a minimal energy configuration for all t, in the sense that its trajectory should follow the ''valleys'' of the free-energy landscape. At given simulation times we define the defect separation r as the distance between the two zeros of ϕ and we measure the total free energy of the system. A potential $V(r)$ for this ''moduli'' is defined by subtracting the energy of two isolated kinks to the energy measured for each value of r in the simulation.

In Figs. 4 and 5 we show $V(r)$ for several values of β, for pairs with opposite and identical charges, respectively.

As expected, the force between opposite charged kinks and antikinks is always attractive. As β increases and the kinks become less localized, the steepness of the potential decreases indicating a weakening of the interaction force. A kink/antikink pair with identical charges displays, on the contrary, a repulsive interaction for distances above a certain threshold. For smaller distances the interaction seems to be always attractive, though results below the core size, $r < l(\beta)$, should not be trusted as the moduli becomes ill-defined. As β increases, the height of the potential maximum becomes larger and its location moves towards smaller values of r. Though for values of β just above the $1/2$ threshold the size of the potential barrier is likely to have negligible effects, as $\beta \to 1$ the kinetic energy needed to surpass the barrier will become increasingly high. As a consequence of the repulsive nature of their interaction, same-charge kinks may be prevented from colliding and we can expect a regime where pair annihilation will be suppressed. As we will see, this will lead to qualitative changes in defect production in a typical phase transition.

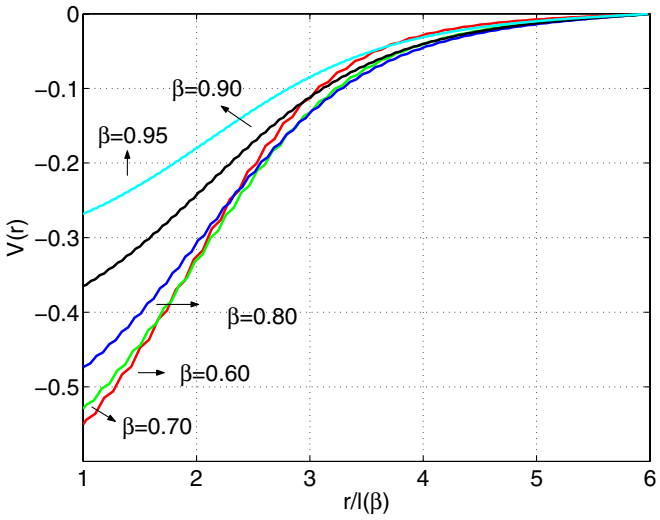

FIG. 4 (color online). The gradient flow interaction potential between a kink and an antikink with opposite charges, for several choices of β. The kink/antikink separation is given in units of core size.

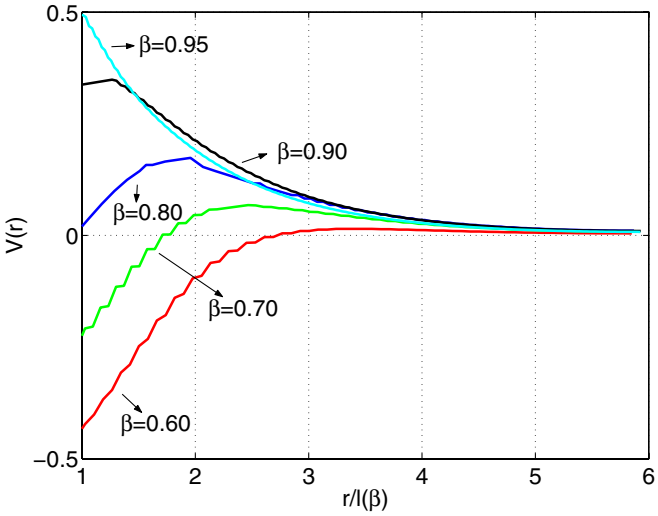

FIG. 5 (color online). Interaction potential for a kink/antikink pair with identical charges, for a selection of values of β. As in Fig. 4, the distance is in terms of the static solution core size.

III. NUMERICAL SIMULATIONS OF DEFECT FORMATION

We now proceed to numerically evaluate the formation of these various types of defects by using a Langevin equation to simulate a series of quenched transitions. Our main goal will be to check whether the types of scaling predicted by the Kibble-Zurek scenario in (2) are compatible with the presence of nontrivial defects as described in the previous section. We will evolve the general second-order Langevin equation

$$\partial_t^2 \phi_a - \partial_x^2 \phi_a + \alpha^2 \partial_t \phi_a + \frac{\partial V}{\partial \phi_a} = \alpha \zeta_a, \tag{18}$$

where the index a runs from 1 to 2 with $\phi_1 = \phi$ and $\phi_2 = \eta$. ζ_a is a Gaussian noise term obeying

$$\begin{aligned} \langle \zeta_a(x', t') \zeta_b(x, t) \rangle &= \Gamma \delta(x' - x) \delta(t' - t) \delta_{ab}, \\ \langle \zeta_a(x, t) \rangle &= 0, \end{aligned} \tag{19}$$

and α measures both the amplitude of the noise and of the dissipative first-order time derivative term. The relation between these two terms ensures that the fluctuation-dissipation theorem is satisfied and guarantees that for very large times thermal equilibrium at temperature $\Gamma/2$ is reached. A simpler version of this model with one single field has been used successfully in several studies of defect formation in $1 + 1$ dimensions [12,47]; we refer the reader

to these for a more detailed discussion of the model and its numerical implementation.

Our goal here is to simulate a "phase transition" with general quench rate τ_Q^{-1}. We start at high temperature with $a > 0$ and, after allowing the fields to equilibrate, we decrease $a(T)$ with T changing according to Eq. (1). As T goes below T_c, a series of defects forms separating regions in alternating vacua. Finally, $a(T)$ settles to a constant negative value and the defect population enters a period of relative slow evolution, with occasional pairs of defects and antidefects annihilating. At this point, we measure the defect density $\rho = 1/\bar{\xi}$ by counting the number of kinks and antikinks in the field configuration. The defects are identified as zero crossings of the ϕ field, suitably coarse-grained over a few lattice sites. The coarse-graining is particularly relevant for high values of β, when the size of the defect core becomes considerably large, and small fluctuations around zero might lead to defect overcounting.

By repeating the above process for several values of the quench rate we obtain $\rho(\tau_Q)$ and fit the results to a power-law $A\tau_Q^{-\sigma}$. Note that depending on the magnitude of the parameter α, Eq. (18) may describe either a relativistic system (small α) or one where dissipation is dominant (large α). The former type of setting will be typical of high-energy and cosmological systems, whereas the later will correspond to condensed-matter systems. As discussed in Section I we should obtain, according to the standard KZ predictions, $\sigma = 1/4$ for the overdamped regime and $\sigma = 1/3$ for the underdamped case.

In Fig. 6 we show σ as a function of β for two choices of α, representative of the two types of regime. In both cases we set $a = 1$, $b = 1$, and $\Gamma = 0.01$, and we vary the quench rate as $\tau_Q = 2^n$, $n = 1, 2, \ldots, 9$. The final defect densities are obtained by averaging over ten independent realizations. Production runs were performed on periodic lattices with 16 000 points and space and time steps of $\delta x = 0.125$ and $\delta t = 0.1$. We found that coarse-graining ϕ over eight lattice points was enough to eliminate any unwanted fluctuations of the field. The error bars, not shown in the plot for clarity, were obtained by calculating the standard deviation over the ensemble of 10 sample runs, and are of order of 10% of the values observed for σ.

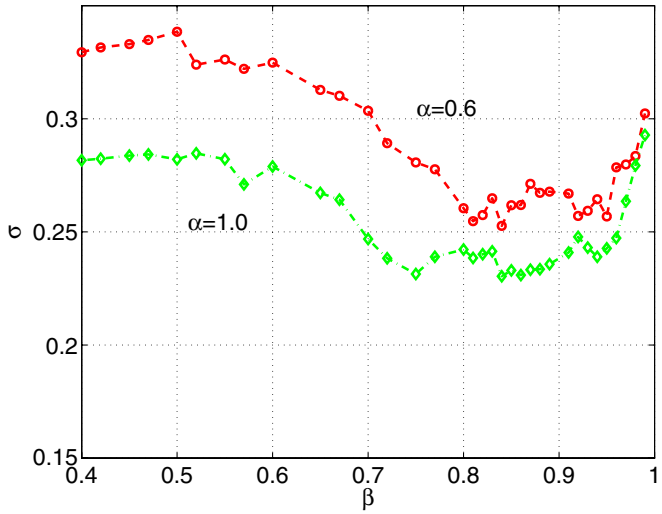

FIG. 6 (color online). The scaling exponent σ as a function of β for $0.4 < \beta < 1$, in the underdamped ($\alpha = 0.6$) and overdamped ($\alpha = 1.0$) regimes. The error bars, not shown for clarity, are of order of 10% of the values measured.

Starting with the high-dissipation results with $\alpha = 1.0$, we see that within error bars, the scaling exponent is approximately constant for $\beta < 0.5$. The value measured $\sigma = 0.28$, coincides with that obtained for similar simulation parameters in the case of a single field system [47]. One should note that the method used to determine the final defect density is known to lead to a slight overestimate in σ when compared to other, computationally more demanding, approaches (for a discussion see [12]). This leads to the deviation from the theoretical prediction $\sigma \sim 1/4$ for the overdamped regime. With this caveat in mind, and remembering that the transition between the under and overdamped regimes is continuous, we will proceed as in [47] and use the value $\sigma \sim 0.30$ to distinguish between the two types of behavior. In the following, all values of σ should be taken in reference to those obtained in the low-β parameter region. As is clear in Fig. 6, as β increases, the scaling exponent goes down signaling a departure from the canonical KZ-scaling behavior, moving deeper into the dissipative regime. For values of β in the vicinity of 0.80, σ reaches a stable plateau, remaining constant (within error bars) up to $\beta \sim 0.97$ when a sharp increase takes place. The results for the relativistic case $\alpha = 0.6$ show a very similar pattern, with σ steadily decreasing towards a flat regime, followed by a sudden rise as $\beta \to 1$.

The initial period of slow decrease in σ for values of β up to 0.7–0.8 can be related to the fact that the effective physical consequences of the dissipation should be measured in terms of the relevant masses of the problem. The relaxation time scale that determines the type of behavior (dissipative vs relativistic) is given by the inverse of α^2/m, where m stands for the lowest mass in the theory. As β increases and $T < T_c$, the mass of one of the excitations of the vacuum approaches zero. When $\beta = 1$ and the original Lagrangian becomes explicitly $U(1)$ symmetric, this degree of freedom corresponds to the massless Goldstone boson. More specifically, the masses of the vacuum excitations for the potential in Eq. (4) are given by $m_1^2 = -2a$ and $m_2^2 = -a(1 - \beta)$. Clearly, m_2 takes increasingly small values as β approaches 1. This leads to a rise in the largest effective dissipation scale α^2/m_2, shifting the system towards the overdamped limit and decreasing the value of σ. In order to check this we simulated a one field relativistic system with a varying mass term. We observed as expected, that as the mass was reduced the value of σ decreased, with the system displaying dissipative effects.

How is this trend towards lower values of the scaling exponent stopped? To understand the overall behavior of σ as displayed is Fig. 6 one must keep in mind that as β takes larger values, the interaction between kinks and antikinks changes considerably. As discussed in Section II B, for large separations, there is a repulsive interaction between kinks and antikinks with the same charge. Note that the effect of the repulsive interaction should not be felt immediately after $\beta > 0.5$, as the height of the potential barrier is initially very small. Nevertheless, since the energy needed to overcome the repulsive barrier increases with β, we expect kink/antikink annihilation to be inhibited for larger values of this parameter. This should lead to survival of a larger number of kink pairs, increasing the final number of defects. What would be the signature of this mechanism in the scaling of the final defect density with quench rate? Clearly the effect would be felt more strongly for fast quenches, where defect densities are higher and annihilation is likely to play a bigger role. An increase in kink survival rates for low values of τ_Q should lead to a steeper distribution $\rho(\tau_Q)$, that is, larger values of the exponent σ.

The mechanism above provides an explanation to why the decrease in σ is halted for values of β roughly halfway between 0.5 and 1.0. In order to confirm this scenario we identified neighboring pairs of kinks and antikinks in the simulation and determined their charges by looking at the sign of η in their cores. Using the knowledge of the spatial distribution of charges at the final time of each simulation, we counted the number of defect pairs with equal and opposite charge, respectively. If same-charge pairs are being prevented from annihilating, then their numbers should be in excess of those of opposite charged pairs. In Fig. 7 we compare the total number (i.e. summed over all quenches) of both types of kink/antikink pairs as a function of β, in the dissipative and relativistic cases. The results match our expectations well, with the fraction of pairs with equal charge deviating little from 0.5 up to values of $\beta \sim 0.7$. Above that threshold there is a decrease in the percentage of pairs with attracting charges, signaling the survival of equal charge pairs due to the rise in the repulsive potential barrier. We also confirmed that this effect is more marked for fast quenches, as discussed above. For reference, the plots include the data of the fraction of pairs with negative charge as well. As expected, as a consequence of the symmetry of the theory, this quantity remains equal to 0.5 within error bars throughout the whole range of β.

Finally we will focus on the apparently anomalous behavior of the system for values of β very near 1, in which limit there is no topological charge. For the three points with highest β, i.e. for $\beta > 0.96$, there is a marked increase in the exponent σ, accompanied by a decrease in the fraction of same-charge pairs. A closer look at the data reveals that the change in relative amount of types of kink/antikink pairs is caused exclusively by the number of pairs with opposite charge going up by a considerable amount. We note that the results for these three values of β should be taken with care since we are in a regime where the kink core size becomes increasingly large. In particular, for fast quenches with high final defect densities, the defect-defect separation becomes of the order of magnitude of the core size. Taking the most extreme case $\beta = 0.99$, we find for the simulation parameters $l = 10$, which implies that each defect has a spatial extension of the order of 20. Our simulation box should in principle not be able to accommodate more than 100 of these kinks, and for fast quenches the number observed is indeed very close (for example 80 in the relativistic case, for the smallest τ_Q). In other words, the correlation length leading to domain formation at the transition is close to the core kink size. These cases should be understood as being effectively in the $U(1)$ regime, with winding springs being formed with no spatially localized core. The dynamics of these objects should be described in terms of unwinding processes and this might lead to a slower annihilation rate than traditional kink/antikink collisions. In terms of the interaction potentials in Fig. 4 this corresponds to the flattening of the attraction potential as $\beta \to 1$. A study of the time scales involved in the departure from equilibrium in such case (using, for example, the techniques developed in [48]) could also shed some light on the dynamics of these systems. A detailed analysis of the unwinding process and its role in defect production in a phase transition will be the focus of a future publication dedicated exclusively to the $U(1)$ theory in $1 + 1$ dimensions [49].

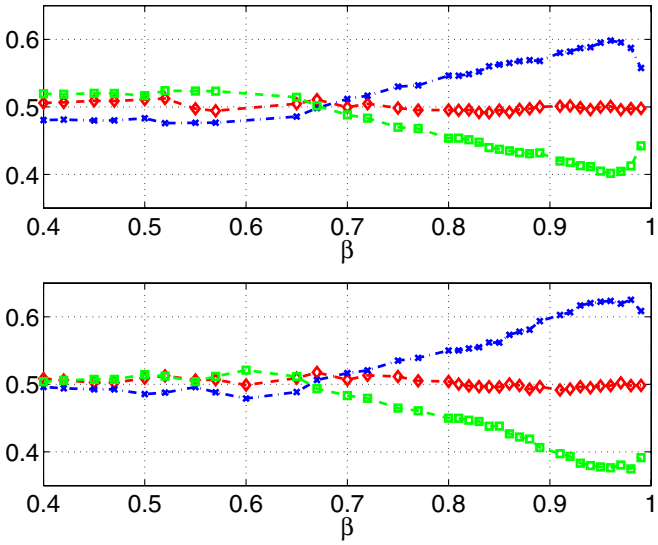

FIG. 7 (color online). Fraction of same-charge kink/antikink pairs (crosses) and opposite charged pairs (squares) as a function of β. For reference we also show the fraction of negative charge kinks (diamonds). The bottom plot corresponds to the underdamped regime $\alpha = 0.6$ and the top plot to the overdamped case $\alpha = 1$.

IV. CONCLUSIONS

We studied kink formation in $1 + 1$ dimensions, in a scalar theory where an added field can lead to condensation in the defect core. We obtained explicit expressions for the nontrivial defect profiles, and determined the region of parameter space for which these are stable. This introduces an extra degree of complexity in the theory as kinks acquire a charge defined in terms of the sign of the core condensate. As a consequence, the process of defect production at a nonequilibrium phase transition suffers a qualitative change, with annihilation of kinks and antikinks being suppressed due to the repulsive nature of their interaction. The degree to which this takes place depends on the parameters of the potential. As a consequence we observed deviations from traditional Kibble-Zurek scaling, with the value of the scaling parameter showing a clear, measurable signature of this effect.

These results open interesting possibilities for the case of higher dimensional theories. Though there seems to be good evidence by now in favor of the stability of vortons in $U(1) \times U(1)$ theories in $3 + 1$ dimensions [50], the question of formation still remains unresolved. Vortons are very fragile objects making a numerical study of their production in a phase transition impossible, the size of the domains required being severely constrained by computational limitations. The model described in this article can be generalized to $2 + 1$ dimensions and an extra condensate field introduced. Such $Z_2 \times U(1)$ theory would display domain walls formed by kinks of the Z_2 field, with the $U(1)$ field condensing in their cores and leading to vortonlike solutions. The lower space-time dimensionality of this model could make numerical simulations of vorton formation possible—a line of research we will be following in a future publication.

ACKNOWLEDGMENTS

N. D. Antunes was funded by PPARC. P. Gandra was supported by FCT, grant number PRAXIS XXI No. BD/18432/98. R. R. would like to acknowledge support from the ESF COSLAB programme.

[1] W. H. Zurek, Nature (London) **317**, 505 (1985); Acta Phys. Pol. B **24**, 1301 (1993).
[2] W. H. Zurek, Phys. Rep. **276**, 177 (1996).
[3] T. W. B. Kibble, Phys. Rep. **67**, 183 (1980).
[4] C. Bauerle *et al.*, Nature (London) **382**, 332 (1996).
[5] V. M. H. Ruutu *et al.*, Nature (London) **382**, 334 (1996).
[6] R. Carmi and E. Polturak, Phys. Rev. B **60**, 7595 (1999).
[7] A. Maniv, E. Polturak, and G. Koren, Phys. Rev. Lett. **91**, 197001 (2003).
[8] R. Monaco, J. Mygind, and R. J. Rivers, Phys. Rev. Lett. **89**, 080603 (2002).
[9] R. Monaco, J. Mygind, and R. J. Rivers, Phys. Rev. B **67**, 104506 (2003).
[10] G. Karra and R. J. Rivers, Phys. Lett. B **414**, 28 (1997).
[11] G. Karra and R. J. Rivers, Phys. Rev. Lett. **81**, 3707 (1998).
[12] P. Laguna and W. H. Zurek, Phys. Rev. Lett. **78**, 2519 (1997).
[13] N. D. Antunes, L. M. A. Bettencourt, and W. H. Zurek, Phys. Rev. Lett. **82**, 2824 (1999).
[14] E. Moro and G. Lythe, Phys. Rev. E **59**, R1303 (1999).
[15] N. D. Antunes, P. Gandra, and Ray J. Rivers, hep-ph/0504004.
[16] M. Hindmarsh and A. Rajantie, Phys. Rev. Lett. **85**, 4660 (2000); A. Rajantie, J. Low Temp. Phys. **124**, 5 (2001).
[17] R. Jeannerot, J. Rocher, and M. Sakellariadou, Phys. Rev. D **68**, 103514 (2003).
[18] M. Sazhin, G. Longo, M. Capaccioli, J. M. Alcalá, R. Silvotti, G. Covone, O. Khovanskaya, M. Pavlov, M. Pannella, M. Radovich, and V. Testa, Mon. Not. R. Astron. Soc. **343**, 353 (2003).
[19] M. Sazhin, O. Khovanskaya, M. Capaccioli, G. Longo, J. M. Alcalá, R. Silvotti, and M. V. Pavlov, astro-ph/0406516.
[20] R. Schild, I. S. Masnyak, B. I. Hnatyk, and V. I. Zhdanov, Astron. Astrophys. **422**, 477 (2004).
[21] G. E. Volovik, *The Universe in a Helium Droplet* (Oxford University, New York, 2003).
[22] G. E. Volovik, V. B. Eltsov, and M. Krusius, cond-mat/0012350.
[23] S. C. Zhang, Science **275**, 1089 (1997); D. Arovas, J. Berlinsky, C. Kallin, and S. C. Zhang, Phys. Rev. Lett. **79**, 2871 (1997).
[24] K. B. W. Buckley and A. R. Zhitnitsky, Phys. Rev. B **67**, 174522 (2003).
[25] D. Vaknin, J. L. Zarestky, and L. L. Miller, Physica C (Amsterdam) **329**, 109 (2000).
[26] B. Lake *et al.*, Science **291**, 1759 (2001); Nature (London) **415**, 299 (2002).
[27] P. Dai *et al.*, Nature (London) **406**, 965 (2000).
[28] V. F. Mitrovic *et al.*, Nature (London) **413**, 501 (2001); V. F. Mitrovic *et al.*, Phys. Rev. B **67**, 220503 (2003).
[29] R. I. Miller *et al.*, Phys. Rev. Lett. **88**, 137002 (2002).
[30] D. B. Kaplan and S. Reddy, Phys. Rev. Lett. **88**, 132302 (2002).
[31] K. B. W. Buckley and A. R. Zhitnitsky, J. High Energy Phys. 08 (2002) 013.
[32] K. B. W. Buckley, M. A. Metlitski, and A R. Zhitnitsky, Phys. Rev. D **68**, 105006 (2003).
[33] M. Alford, K. Rajagopal, and F. Wilczek, Phys. Lett. B **422**, 247 (1998); R. Rapp, T. Schäfer, E. V. Shuryak, and M. Velkovsky, Phys. Rev. Lett. **81**, 53 (1998); K. Rajagopal and F. Wilczek, *At the Frontier of Particle Physics/Handbook of QCD*, edited by M. Shifman (World

Scientific, Singapore, 2001), Chap. 35.
[34] E. Witten, Nucl. Phys. **B249**, 557 (1985).
[35] E. J. Copeland, N. Turok, and M. Hindmarsh, Phys. Rev. Lett. **58**, 1910 (1987).
[36] C. T. Hill, H. M. Hodges, and M. S. Turner, Phys. Rev. D **37**, 263 (1988).
[37] R. L. Davis, Phys. Rev. D **38**, 3722 (1988).
[38] R. L. Davis and E. P. S. Shellard, Nucl. Phys. **B323**, 209 (1989).
[39] M. A. Metlitski and A. R. Zhitnitsky, J. High Energy Phys. 06 (2004) 017.
[40] R. MacKenzie, M. A. Vachon, and U. F. Wichoski, Phys. Rev. D **67**, 105024 (2003).
[41] S-C. Zhang, Science **275**, 1089 (1997).
[42] D. P. Arovas, A. J. Berlinsky, C. Kallin, and S-C. Zhang, Phys. Rev. Lett. **79**, 2871 (1997).
[43] S. Alama, A. J. Berlinsky, L. Brossard, and T. Giorgi, Phys. Rev. B **60**, 6901 (1999).
[44] N. D. Antunes and T. Vachaspati, Phys. Rev. D **70**, 063516 (2004); N. D. Antunes, L. Pogosian, and T. Vachaspati, Phys. Rev. D **69**, 043513 (2004); L. Pogosian and T. Vachaspati, Phys. Rev. D **64**, 105023 (2001); **62**, 123506 (2000).
[45] Th. Busch and J. R. Anglin, Phys. Rev. Lett. **87**, 010401 (2001).
[46] N. S. Manton, Phys. Rev. Lett. **60**, 1916 (1988).
[47] N. D. Antunes, P. Gandra, and Ray J. Rivers, Phys. Rev. D **71**, 105006 (2005).
[48] C. J. Gagne and M. Gleiser, Physica D (Amsterdam) **181**, 121 (2003).
[49] N. D. Antunes, P. Gandra, Ray J. Rivers, and A. Swarup (unpublished).
[50] Y. Lemperiere and E. P. S. Shellard, Phys. Rev. Lett. **91**, 141601 (2003).